

Controllable Evolution of NiOOH/Au³⁺ Active Species for the Oxidation of 5-Hydroxymethylfurfural

Xuliang Pang ^{a,b*}, Yifei Huang ^a, Huaiquan Zhao ^a, Weiqiang Fan ^{a*}, Hongye Bai ^{a*}

^a *School of Chemistry and Chemical Engineering, Jiangsu University, Zhenjiang, 212013, P. R. China.*

^b *Shandong Provincial Key Laboratory of Monocrystalline Silicon Semiconductor Materials and Technology, Dezhou University, Dezhou 253023, PR China*

E-mail: pangxuliang163@163.com, bhy198412@163.com, fwq4993329@ujs.edu.cn

Experimental

Chemicals

HMF, 5-hydroxymethyl-2-furancarboxylic acid (HMFCFA), 5-formyl-2-furancarboxylic acid (FFCA) and furan-2, 5-dicarbaldehyde (DFF) and FDCA were purchased from Aladdin. All other chemicals and reagents were obtained from Sinopharm Chemical Reagent Co., Ltd in China.

Synthesis

Firstly, Ni-BTC MOF was prepared on copper foam (CF) by electrochemical deposition. Under constant stirring, 1.1 g 1, 3, 5-benzenetricarboxylic acid, 1.6 g methyltributylammonium methyl sulfate and 0.65 g $\text{Ni}(\text{NO}_3)_2 \cdot 6\text{H}_2\text{O}$ were dissolved in 50 mL DMF to obtain electrodeposition solution. Electrodeposition potential: -1.5 V vs. Ag/AgCl, electrodeposition time: 800 s. Finally, the prepared CF-Ni MOF sample was washed with deionized water. Secondly, under vigorous stirring, dilute NaBH_4 solution (1 mg/L) was slowly added to 50 mL HAuCl_4 solution (0.5 mM) until the solution was burgundy. The prepared CF-Ni MOF was soaked in the above solution for 5 min, washed with deionized water and dried in a vacuum drying oven.

Characterization

The micro-morphology of samples was obtained by scanning electron microscopy (SEM, Apreo S HiVac). The valence-state and contents of samples were measured by X-ray photoelectron spectroscopy (XPS, Physical Electrons Quantum 2000 Scanning Esca Microprobe). The crystalline phases of samples were determined by (XRD, Bruker D8 Advance X-ray diffractometer).

Electrochemical measurements

Electrochemical tests (cyclic voltammetry (CV), linear sweep voltammetry (LSV), electrochemical impedance spectroscopy (EIS) and open-circuit voltage-time (OCPT)

were conducted in an H-shaped electrolytic cell. Activated CF-Ni MOF/Au was used as the working electrode, Ag/AgCl and Pt wire electrodes were used as the reference electrode and counter electrode, respectively. The electrolyte was 1.0 M KOH (pH 14.0), and the scanning rate was 5 mV/s. The frequency range of electrochemical impedance measurement is 0.1–10⁶ Hz.

The oxidative activation of the Ni MOF/Au catalyst was mainly accomplished in two steps. First, the catalyst Ni MOF/Au was subjected to three consecutive LSV scans in 1.0 M KOH. Subsequently, another 120 cycles of CV scanning were performed to ensure that the catalyst surface had been completely oxidized to high-valence NiOOH/Au³⁺ species.

HPLC analysis

The quantitative analysis of HMF and products was recorded on high performance liquid chromatography (HPLC, Shim-pack GWS C-18 column: 5.0 μm*4.6 mm*150 mm). Detection wavelength: 265 nm, Column temperature: 40°C. Mobile phase A: 70% ammonium formate (5.0 mM), Mobile phase B: 30% methanol. Flow rate: 0.6 mL/min. 20 μL sample was diluted to 2 mL as HPLC test solution. HMF conversion, FDCA yield and Faradaic efficiency (FE) were calculated using the following equations. *F* (96485 C/mol) represents Faraday's constant.

$$\text{HMF conversion} = \frac{\text{Consumed HMF}}{\text{Initial HMF}} \times 100\%$$

$$\text{FDCA yield} = \frac{\text{Formed FDCA}}{\text{Initial HMF}} \times 100\%$$

$$\text{FE of FDCA} = \frac{\text{Formed FDCA}}{\text{Consumed charge}/(6 \times F)} \times 100\%$$

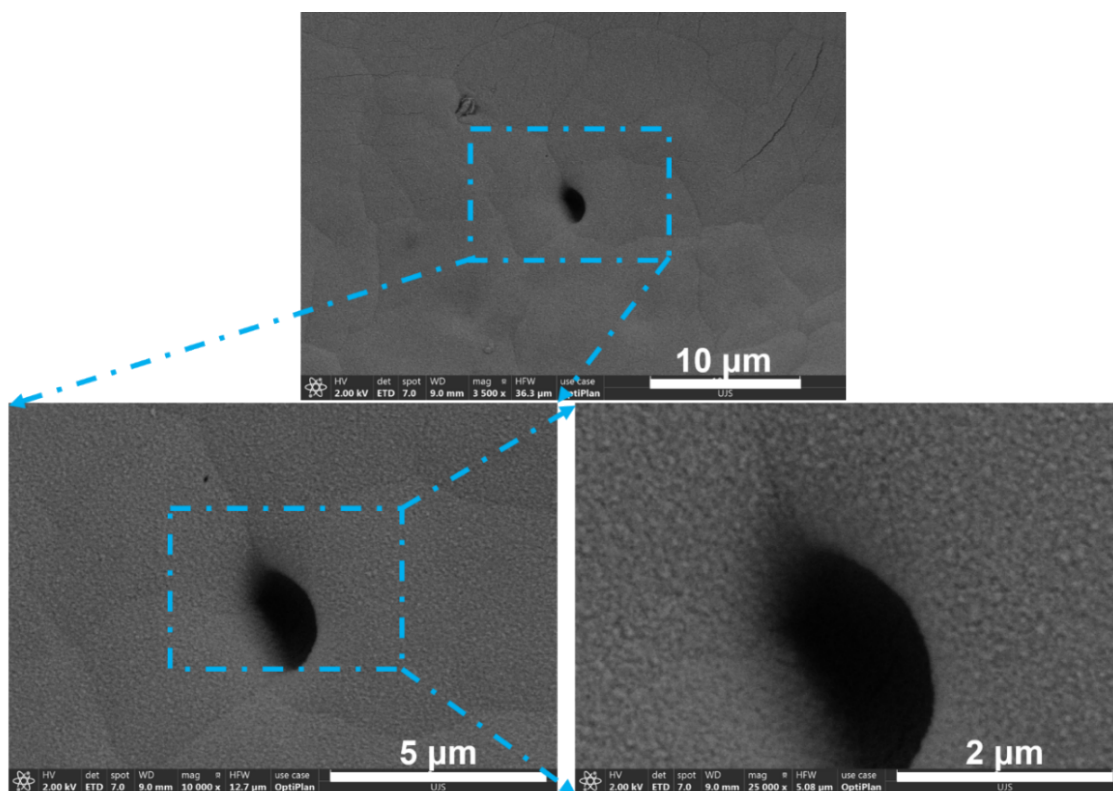


Fig. S1. SEM images of CF-Ni MOF.

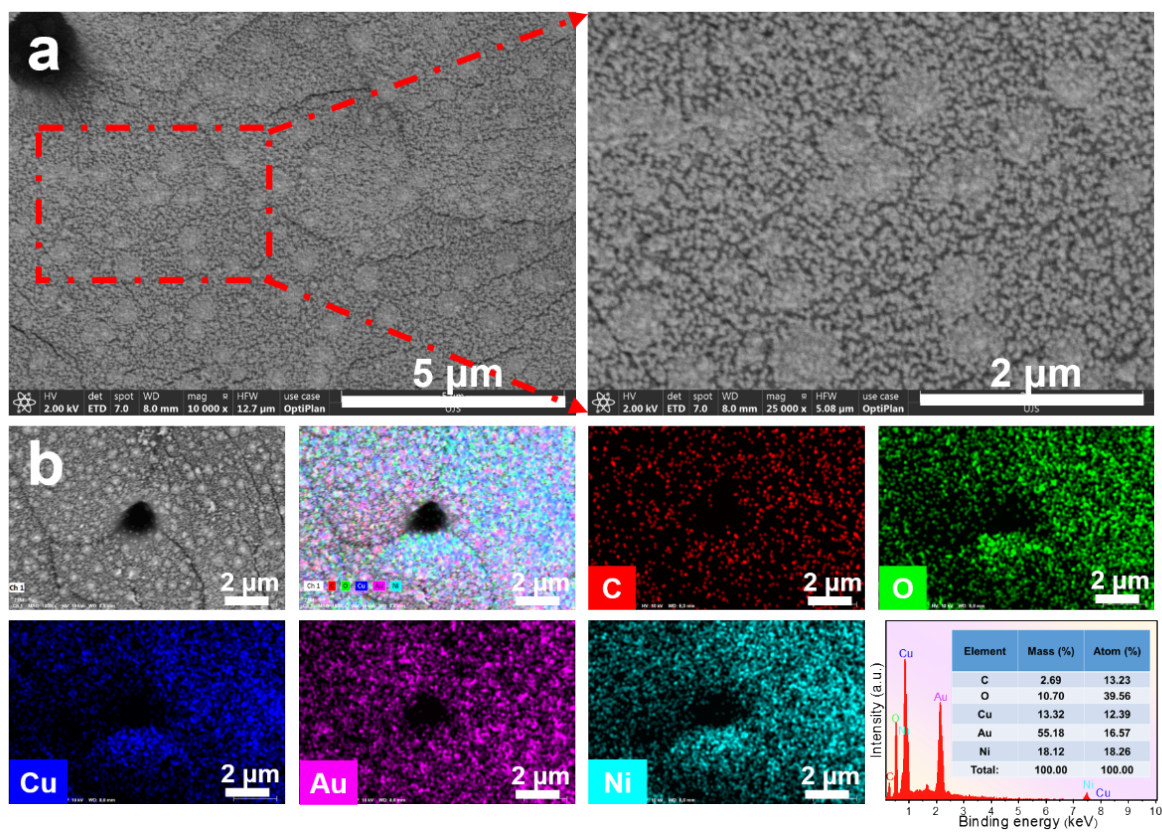


Fig. S2. SEM (a) and EDS-mapping (b) images of the activated CF-Ni MOF/Au.

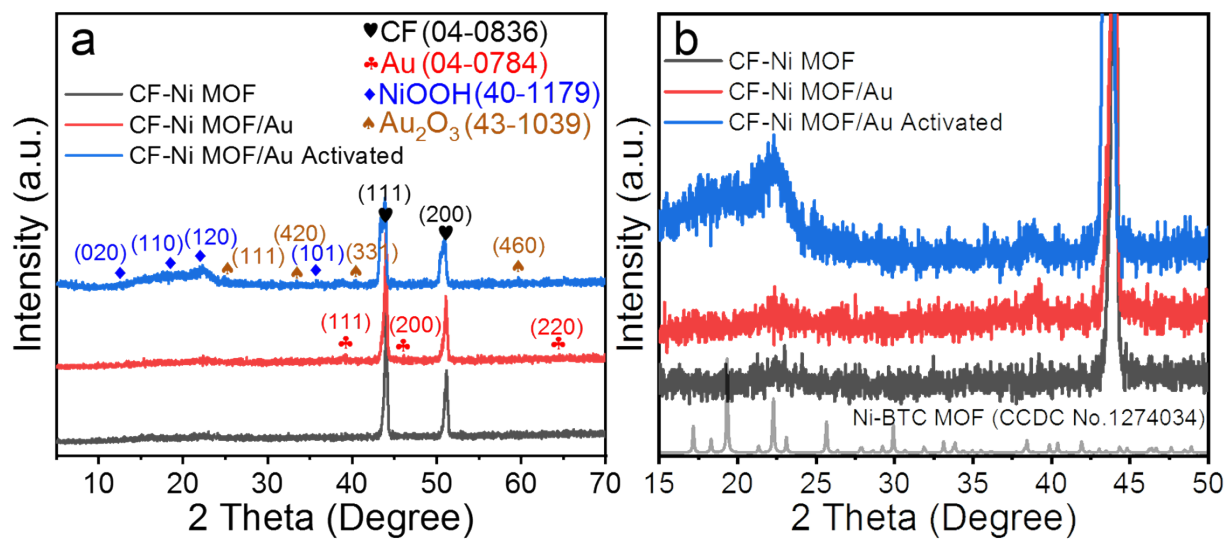


Fig. S3. XRD patterns of CF-Ni MOF, CF-Ni MOF/Au, activated CF-Ni MOF/Au (a). The partially enlarged view for XRD patterns (b).

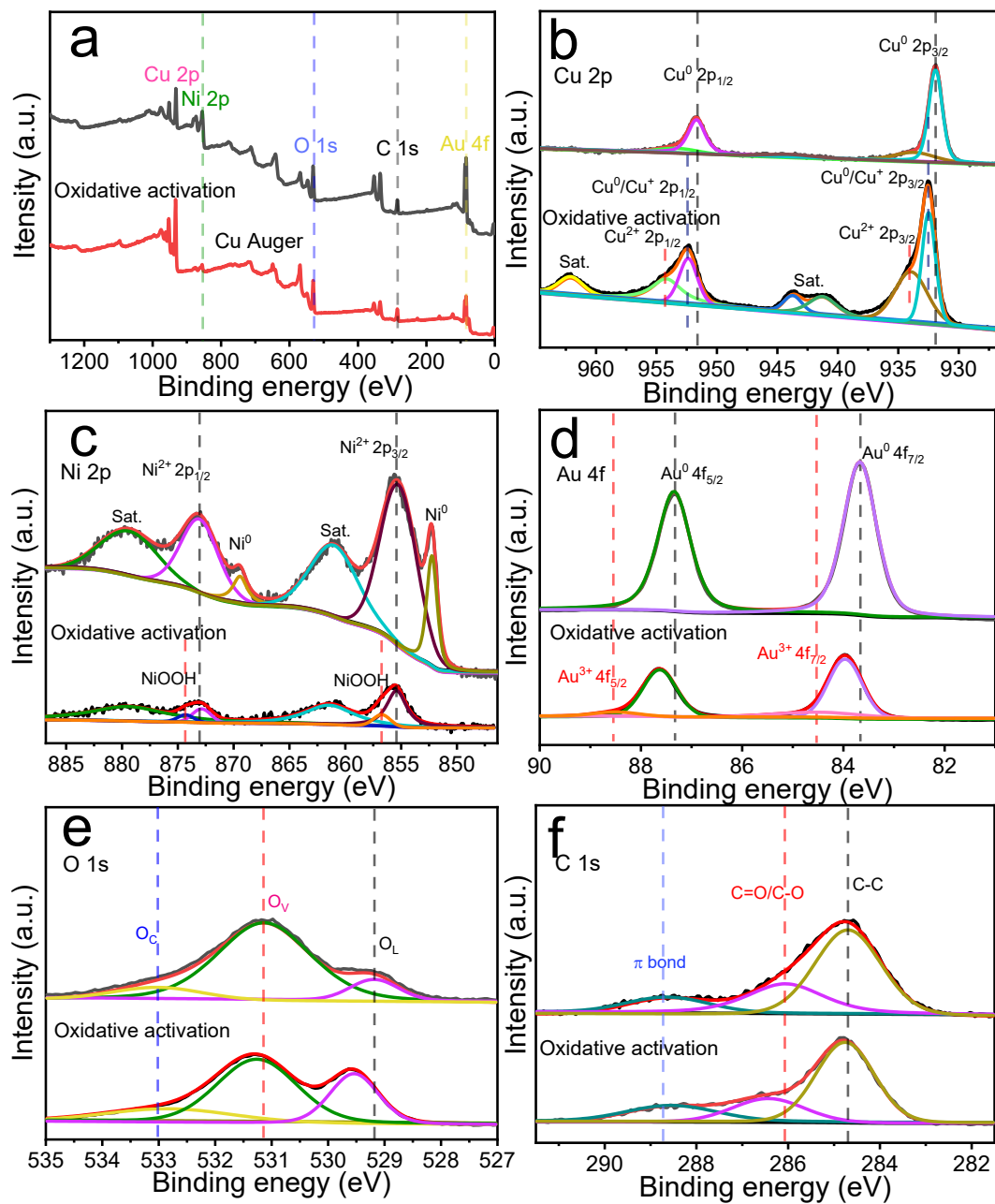


Fig. S4. Full-scan XPS spectra of CF-Ni MOF/Au and activated CF-Ni MOF/Au (a). XPS spectra of Cu 2p (b), Ni 2p (c), Au 4f (d), O 1s (e) and C 1s (f) of CF-Ni MOF/Au and activated CF-Ni MOF/Au.

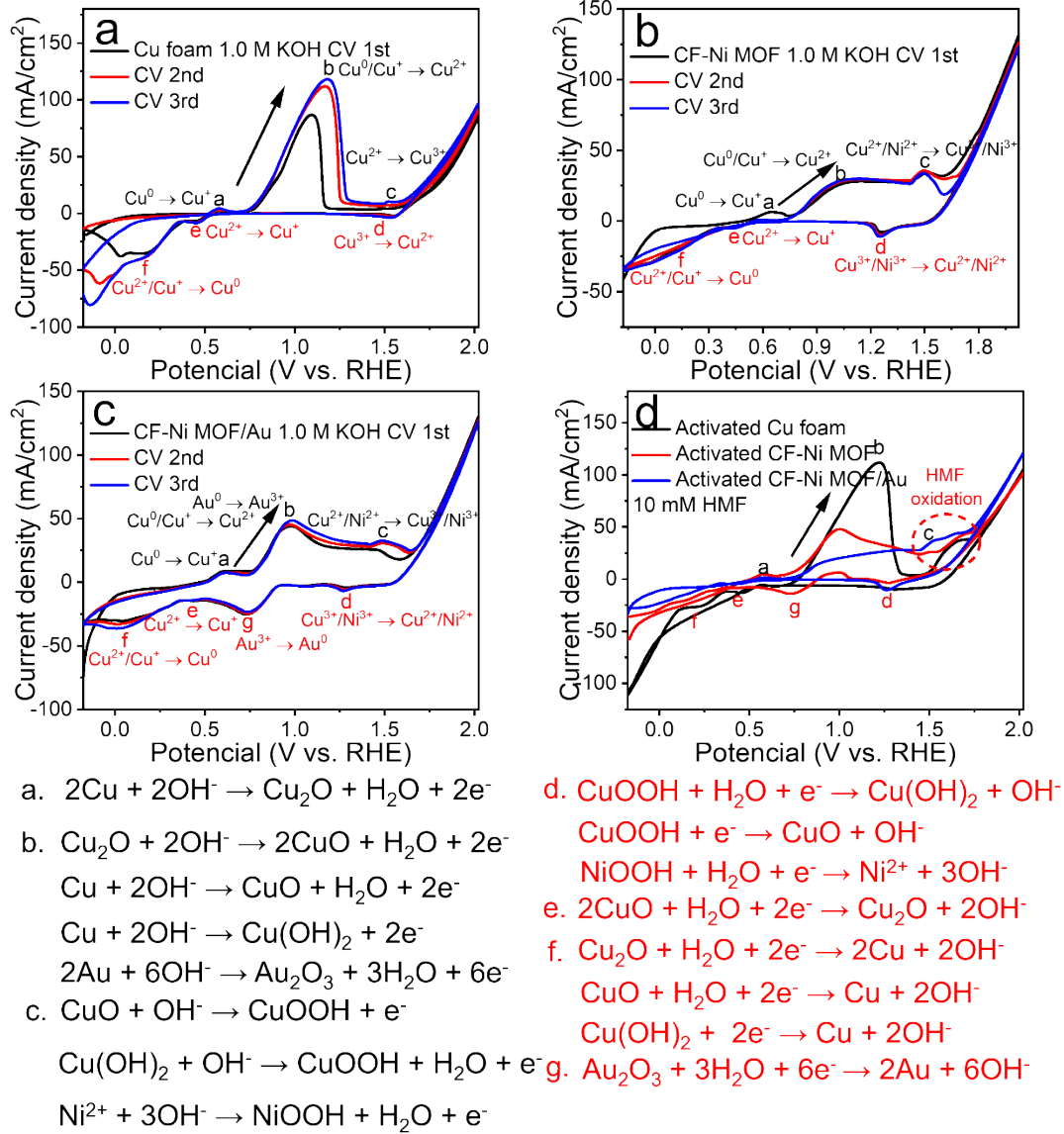


Fig. S5. CV curves of Cu foam (a), CF-Ni MOF (b) and CF-Ni MOF/Au (c) in 1.0 M KOH solution. CV curves of Cu foam, CF-Ni MOF and CF-Ni MOF/Au in the presence of 10 mM HMF (d). (Scan rate: 5 mV/s).

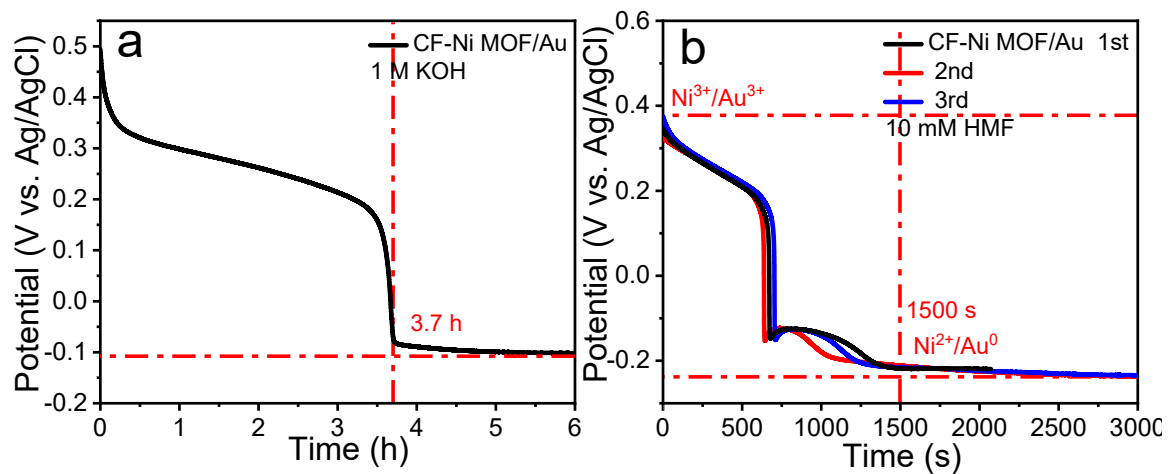


Fig. S6. OCPT of CF-Ni MOF/Au in 1.0 M KOH solution (a). Three consecutive OCPTs of CF-Ni MOF/Au in 10 mM HMF (b).

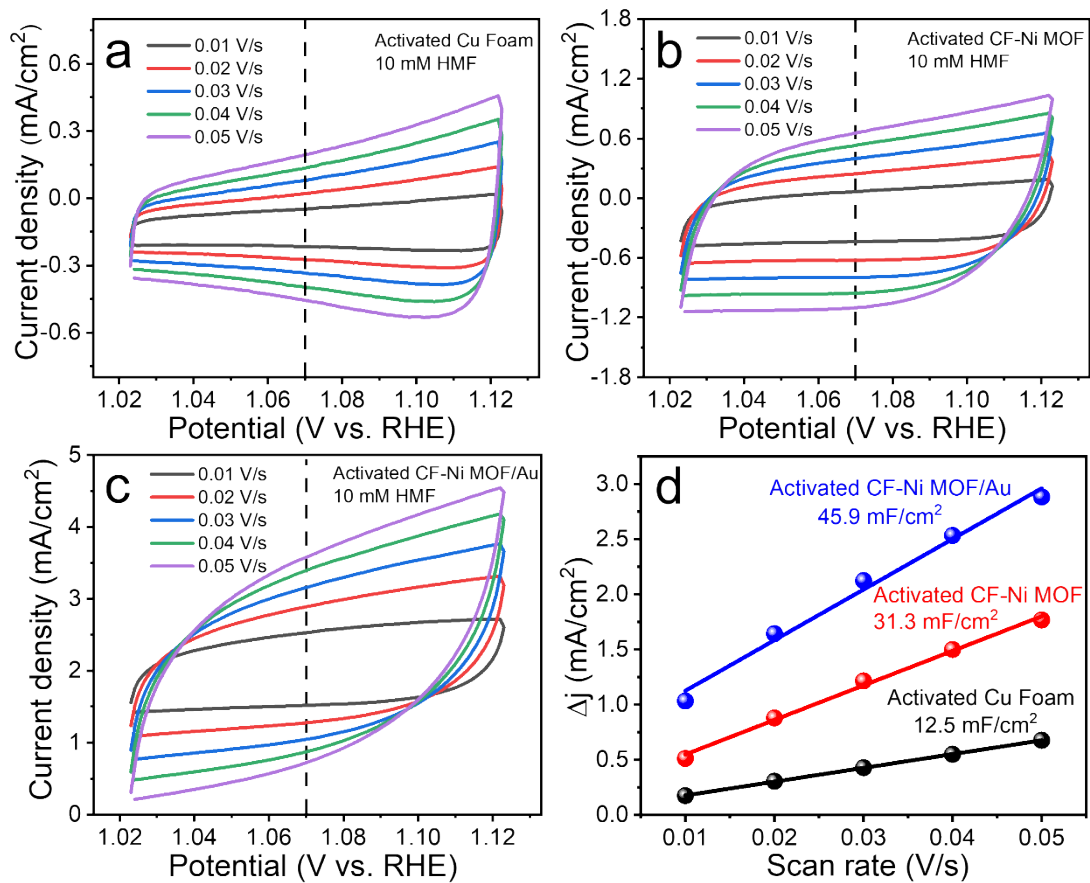


Fig. S7. CV curves of the activated CF (a), CF-Ni MOF (b) and CF-Ni MOF/Au (c) in the presence of 10 mM HMF at different scan rates. Current density vs. scan rates (d).

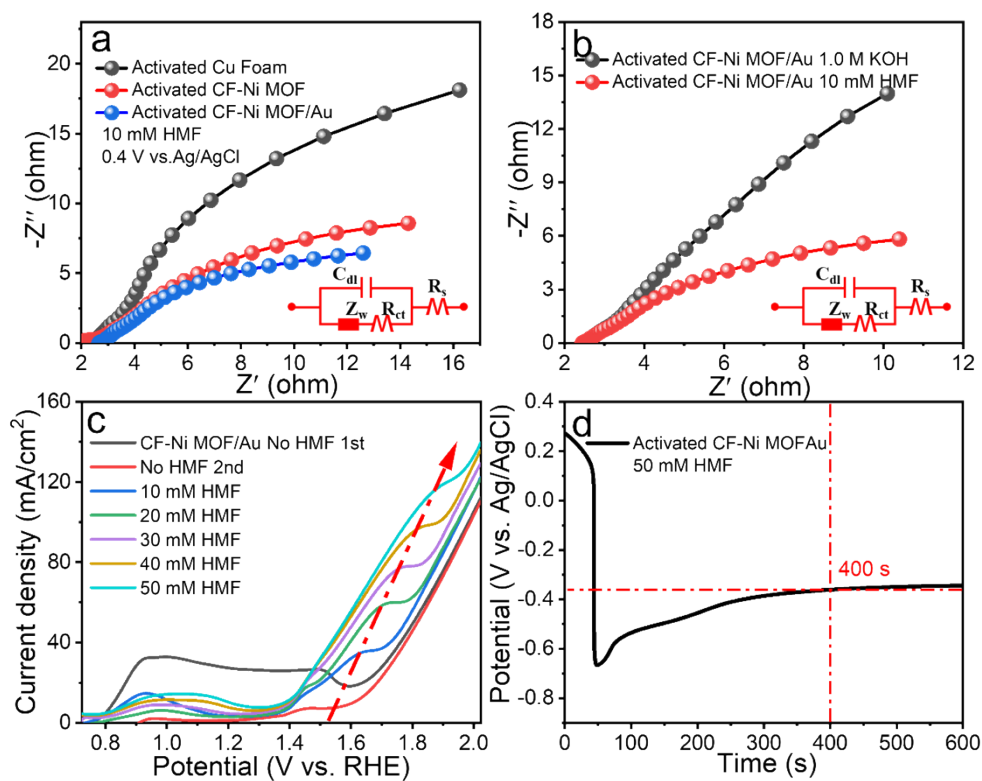


Fig. S8. EIS plots (1.42 V vs. RHE) of CF, CF-Ni MOF and CF-Ni MOF/Au in the presence of 10 mM HMF (a). EIS plots (1.42 V vs. RHE) of CF-Ni MOF/Au in the absence or presence of 10 mM HMF (b). LSV curves of CF-Ni MOF/Au at different concentration of HMF (c). OCPT experiment of the activated CF-Ni MOF/Au in the presence of 50 mM HMF (d).

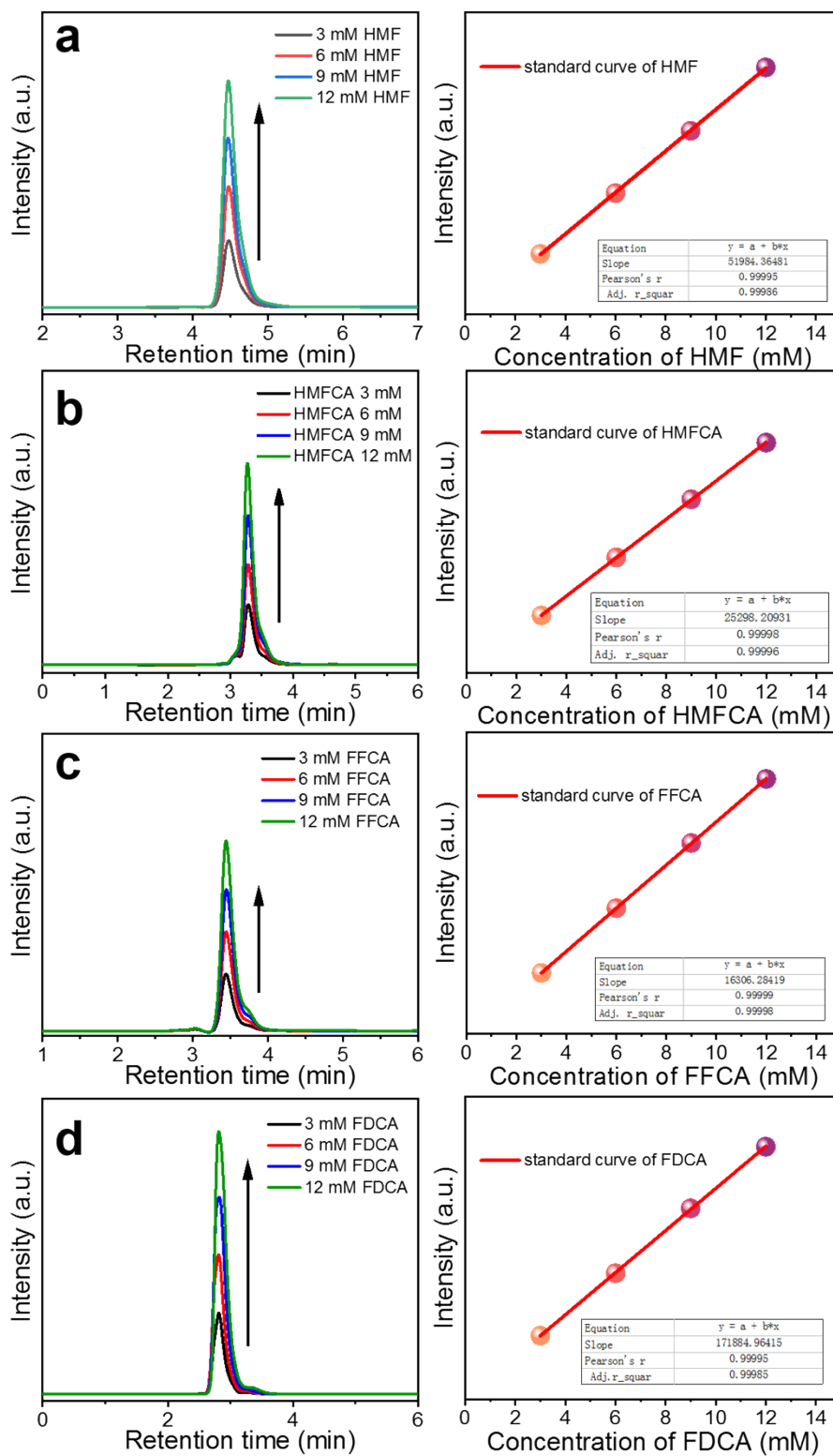


Fig. S9. Calibration curves of HMF (a), HMFCFA (b), FFCA (c) and FDCA (d).

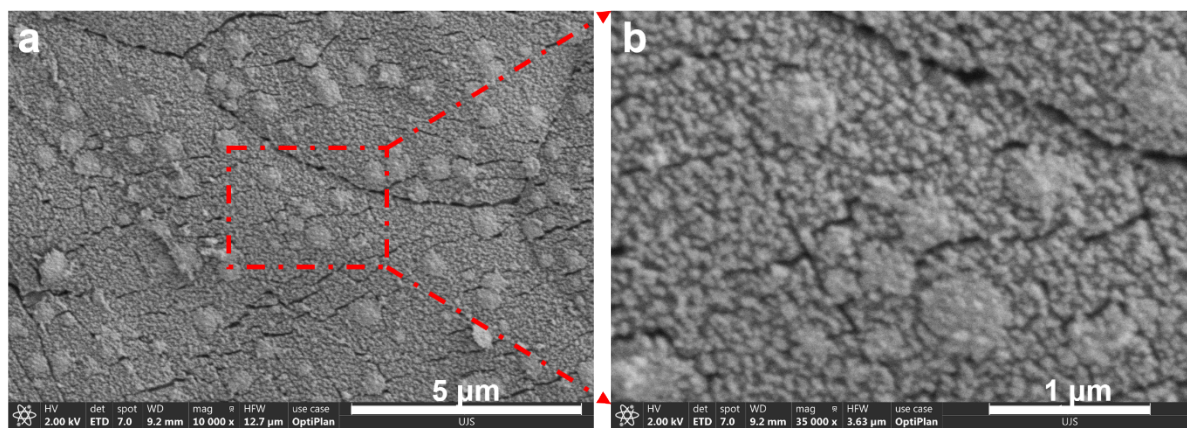


Fig. S10. SEM images of the activated CF-Ni MOF/Au after the five successive electrocatalytic HMF oxidations.

Fig. S11. Electrocatalytic mechanism of NiOOH/Au³⁺ species for HMF oxidation.